Structural Analysis of Immunotherapeutic Peptides for Autoimmune Myasthenia Gravis[†,‡]

Hyun Ho Jung, Hwa Jung Yi, Seung Kyu Lee, Ju Yeon Lee, Hoi Jong Jung, Sung Tae Yang, Young-Jae Eu, Sin-Hyeog Im,* and Jae Il Kim*

Department of Life Sciences, Research Center for Biomolecular Nanotechnology, Gwangju Institute of Science and Technology, Gwangju 500-712, Korea

Received July 2, 2007; Revised Manuscript Received October 20, 2007

ABSTRACT: Myasthenia gravis (MG) and its animal model, experimental MG (EAMG), are autoimmune disorders in which major pathogenic antibodies are directed against the main immunogenic region (MIR) of the nicotinic acetylcholine receptor (nAChR). In an earlier attempt to develop peptide mimotopes capable of preventing the anti-MIR-mediated pathogenicity, the peptide Pep.1 was initially identified from phage display, and subsequently, Cyclic extended Pep.1 (Cyc.ext.Pep.1), which incorporates eight additional residues into the Pep.1 sequence and has an affinity for the anti-MIR antibody mAb198 3 orders of magnitude greater than that of Pep.1, was developed. In an animal model, Pep.1 shows no ability to inhibit mAb198-induced EAMG, whereas Cyc.ext.Pep.1 successfully blocks anti-MIR antibody 198 (mAb198)-induced EAMG. Our aim in this study was to identify the structural characteristics related to the different affinities for mAb198 of Pep.1 and Cyc.ext.Pep.1 using NMR spectroscopy and alanine scanning analysis. The NMR structural analysis revealed that Pep.1 is very flexible in solution, whereas Cyc.ext.Pep.1 is highly rigid within a region containing several turn structures. Interestingly, TRNOE experiments revealed that mAb198-bound Pep.1, particularly in the region between Asn7 and Glu11, shows significant structural similarity to the region between Asn10 and Glu14 of Cyc.ext.Pep.1, which is critical for interaction with mAb198. We therefore conclude the higher affinity of Cyc.ext.Pep.1 for mAb198 reflects the fact that incorporation of additional residues producing a single disulfide bond endows Pep.1 with a conformational rigidity that mimics the structure of mAb198-bound Pep.1. Furthermore, our results suggest that cyclic extended peptides could be utilized generally as useful tools to optimize the affinity of phage library-derived peptide antigens.

MG[1] and its experimental model, EAMG, are T-cell-dependent antibody-mediated autoimmune diseases manifested by muscle weakness and fatigue. In both cases, nAChRs at the neuromuscular junction are the major autoantigens. EAMG, which mimics human MG in its clinical and immunological manifestations and has been used as a reliable model with which to investigate therapeutic strategies for the treatment of MG, can be induced in animals by passive transfer of the anti-nAChR antibody mAb198 or by active immunization of purified nAChR (*1*, *2*). Although the antibody response to nAChR in MG is heterogeneous, ∼60% of the pathogenic anti-nAChR antibodies are directed against the well-defined MIR, corresponding to residues 67−76 in the extracellular domain nAChR α-subunit. Given the importance of the MIR in the pathogenicity of MG, much effort has been directed toward developing immunoneutralizing peptide analogues of the MIR sequence (*3*−*6*). Despite this effort, however, no breakthrough has been made, in large part because almost all of the antibodies are conformation-specific; consequently, they mimic the natural conformational epitope only through sequential determinants, which limits their ability to inhibit the autoimmune attack on nAChRs.

[†]This research was supported by grants from the 21C Frontier Functional Human Genome Project, the Neurobiology Research Program from the Korea Ministry of Science and Technology, the KBRDG initiative research program, the regional technology innovation program of the MOCIE (Grant RTI05-01-01), the SRC/ERC program of MOST/KOSEF (R11-2000-083-00000-0), the Brain Research Center of the 21st Century Frontier Research Program (M103KV010005-06K2201-00510), a Next Generation New Technology Development Program Grant (10027891) from MOCIE, and the Development of Marine Novel Compounds Program of the Korean Ministry of Maritime Affairs and Fisheries.

[‡]Atomic coordinates for the converged structures of mAb198-bound Pep.1 and Cyc.ext.Pep.1 have been deposited in the Protein Data Bank as entries 2jrv and 2jrw, respectively.

* To whom correspondence should be addressed. J.I.K.: Department of Life Sciences, Room 106, Gwangju Institute of Science and Technology, Gwangju 500-712, Korea; telephone, 82-62-970-2494; fax, 82-62-970-2484; e-mail, jikim@gist.ac.kr. S.-H.I.: telephone, 82-62-970-2503; fax, 82-62-970-2484; e-mail, imsh@gist.ac.kr.

[1] Abbreviations: NOE, nuclear Overhauser effect; TRNOE, transferred NOE; NOESY, NOE spectroscopy; NMR, nuclear magnetic resonance; PDB, Protein Data Bank; rms, root-mean-square; RP-HPLC, reversed-phase high-performance liquid chromatography; TFA, trifluoroacetic acid; TOCSY, total correlation spectroscopy; PBS, phosphate-buffered saline; mAb, monoclonal antibody; DQF-COSY, double-quantum-filtered correlation spectroscopy; Fmoc, 9-fluorenylmethoxycarbonyl; MALDI-TOF, matrix-assisted laser desorption ionization time-of-flight; nAChR, nicotinic acetylcholine receptor; MG, myasthenia gravis; EAMG, experimental autoimmune myasthenia gravis; MIR, main immunogenic region; hMIR, human MIR; DIC, 1,3-diisopropylcarbodiimide; HOBt, 1-hydroxybenzotriazole; NMP, *N*-methylpyrrolidone; Cyc.ext.Pep.1, cyclic extended Pep.1; mAb198, monoclonal antipeptide antibody 198; ODS, octadecylsilica.

10.1021/bi701298b CCC: $37.00
Published on Web 12/01/2007

Table 1: Amino Acid Sequences of hMIR, Pep.1, and Cyc.ext.Pep.1

name	sequence
hMIR fragment	WNPDDYGGIK
Pep.1	PMTLPENYFSERPYH
Cyc.ext.Pep.1	CAE PMTLPENYFSERPYH PPPPC

In an effort to find neutralizing peptide ligands for target proteins such as autoantibodies, phage display technology has been successfully used to screen peptide mimotopes with high affinity for target molecules. In collaboration with Venkatesh et al., we previously identified a candidate immunotherapeutic peptide for MG (Pep.1) through the screening of phage epitope libraries. Pep.1 is a 15-mer peptide (PMTLPENYFSERPYH) that specifically binds to mAb198 and competitively inhibits its binding to nAChR. However, the affinity of Pep.1 for mAb198 proved to be too low to inhibit mAb198-mediated EAMG in rats. To increase the affinity by mimicking the conformation of the phage construct, eight flanking residues, including terminal cysteine residues, were incorporated at both ends, yielding Cyc.ext.Pep.1 (CAEPMTLPENYFSERPYHPPPPC). Cyc.ext.Pep.1 has an affinity for mAb198 3 orders of magnitude greater than that of Pep.1 and the ability to competitively inhibit its binding to the nAChR (*3*). The structural basis for the increased affinity of Cyc.ext.Pep.1 remained unknown, however.

In this study, we carried out NMR structural analysis to compare the structures of Pep.1 and Cyc.ext.Pep.1 and alanine-scanning functional analysis of Pep.1 to define the factors underlying the difference in the affinities of Pep.1 and Cyc.ext.Pep.1 for mAb198. In addition, to assess the structure of the antigen epitope within the nAChR, the structure of mAb198-bound Pep.1 was determined using TRNOE (*7*−*11*). Through the structural comparison between Cyc.ext.Pep.1 and mAb198-bound Pep.1, we reveal the structural mechanism underlying the affinity maturation that occurs upon going from Pep.1 to Cyc.ext.Pep.1.

MATERIALS AND METHODS

Peptide Synthesis. Pep.1, analogues of Pep.1 for alanine scanning, a linear precursor of Cyc.ext.Pep.1, and hMIR (residues 67−76 of the human nAChR α-subunit) were synthesized using the solid-phase method of Fmoc chemistry (*12*). Table 1 shows the sequence of each peptide. Fmoc (9-fluorenylmethoxycarbonyl) resins and amino acids were purchased from Novabiochem, DIC (1,3-diisopropylcarbodiimide) and HOBt (1-hydroxybenzotriazole) from Iris Biotech (Marktredwitz, Germany), and piperidin and NMP (*N*-methylpyrrolidone) from Dae-Jung Chemicals (Siheung, Korea). Peptide synthesis was started from Fmoc-His-Alko resin, Fmoc-Ala-Alko resin, Fmoc-Cys-Alko resin, or Fmoc-Lys-Alko resin using a variety of blocking groups to protect the amino acids. A coupling reaction for each amino acid was performed for 3 h at 25 °C using DIC/HOBt reagents. Fmoc cleavage for each redsidue was performed twice (5 or 10 min) with 20% piperidine in NMP at 25 °C. Once synthesis was complete, the protection was removed from the synthetic peptides, which were then cleaved using a mixture containing 82.5% TFA (trifluoroacetic acid), 2.5% 1,2-ethanedithiol, 5% H_2O, 5% thioanisole, and 5% phenol for 4 h at 25 °C, and precipitated with diethyl ether. For the folding of Cyc.ext.Pep.1, the crude linear peptide was diluted to a final concentration of 100 μM and stirred in PBS (phosphate-buffered saline) (pH 7.0) at 4 °C for 1 day. The folding reaction was checked by 23% isocratic RP-HPLC through comparison to linear Pep.1. Purification of each peptide was conducted using a Shimadzu LC-6AD system equipped with an ODS (octadecylsilica) column (20 mm × 250 mm) and confirmed by analytical RP-HPLC and MALDI-TOF mass spectrometry. Finally, both Pep.1 and Cyc.ext.Pep.1 were obtained in 19.1 and 8.1% yields, respectively.

Monoclonal Antipeptide Antibody 198 (mAb198). mAb198, which was kindly provided by S. J. Tzartos (*6*), is an IgG2a anti-MIR mAb derived from rat immunized with intact nAChR isolated from human muscle and binds to the MIR of nAChRs in both human and rat muscle and in the *Torpedo* electric organ.

NMR Spectroscopy for Pep.1 and Cyc.ext.Pep.1. For NMR experiments with Pep.1, samples were prepared at a concentration of 1 mM in PBS [90% H_2O/10% D_2O (v/v), pH 6.1], and the experiments were carried out in the presence or absence of mAb198 on a Bruker DRX 600 spectrometer with TXI probe. To determine the molar ratio of mAb198 and Pep.1 for TRNOE measurements, one-dimensional spectra were recorded at a variety of peptide:antibody binding site ratios (8:1, 10:1, 15:1, 20:1, 30:1, and 40:1). The most appropriate ratio for TRNOE measurements was determined to be 10:1, which meant combining 1 mM peptide with 50 μM antibody (100 μM binding site). All two-dimensional (2D) NMR measurements were conducted using a phase-sensitive mode with time-proportional phase incrementation at 298 K (*13*). TOCSY spectra were recorded using a MLEV-17 pulse scheme with isotropic mixing times of 80 ms (*14*). NOESY spectra were recorded with mixing times of 100−300 ms (*15*, *16*). Water suppression in both the NOESY and TOCSY experiments was achieved using the WATERGATE scheme (*17*). DQF-COSY spectra were recorded to obtain the constraints for the torsion angles and stereospecific assignments (*18*). The data were acquired with a 90° pulse of 12.5 μs and a sweep width of 7002 Hz, which were in size 256 (t_1) × 2048 (t_2) for TOCSY and 512 × 2048 for others. The acquistion time of TOCSY was 5 h, and those of others were 11 h. Chemical shifts were referred to internal TSP. XWINNMR and ANSIG were used for processing and analysis of the spectra. Phase-shifted sine-squared window functions were applied before Fourier transformation. The data were zero-filled twice to give 512 × 2048 real points for TOCSY and 1024 × 2048 real points for others.

All NMR measurements for Cyc.ext.Pep.1 were performed, using standard pulse sequences and phasing cycling, at 1 mM, pH 3.1, and 288 K (90% H_2O/10% D_2O) (*13*). NOESY spectra were acquired with mixing times of 100, 200, 250, and 300 ms (*15*, *16*). All other NMR experiments were carried out in the same way as for Pep.1.

Calculation of the Structures of mAb198-Bound Pep.1 and Cyc.ext.Pep.1. The intensities of cross-peaks were determined quantitatively on the basis of the counting levels. Transferred NOEs in the case of to mAb198-bound Pep.1 and NOE data for Cyc.ext.Pep.1 were classified into four distance ranges: 1.8−2.7, 1.8−3.5, 1.8−5.0, and 1.8−6.0 Å, corresponding to strong, medium, weak, and very weak values, respectively.

Pseudoatoms were used for the methyl protons or the nonstereospecifically assigned methylene protons (*19*). For the use of pseudoatoms, correcting factors were added to the distance constraints (*20*). The backbone NH−CαH coupling constants were measured from the DQF-COSY spectrum and were translated to backbone torsion angle constraints according to the following rules. For $^3J_{NH-C\alpha H}$ values of <5.5 Hz, the angle was constrained in the range of −65 ± 25°; for $^3J_{NH-C\alpha H}$ values of >8.0 Hz, the angle was constrained in the range of −120 ± 40° (*21*, *22*). Calculation of the structures of both peptides was carried out using X-PLOR version 3.851 (*23*). The three-dimensional structures were calculated on the basis of the distance and torsion angle constraints derived from the NMR spectra using a dynamically simulated annealing protocol. On the basis of the minimum overall energy and Lennard-Jones van der Waals energy, the final 20 structures were chosen for structural analysis. The structural analysis of both peptides was carried out using PROCHECK_NMR (*24*) and PROMOTIF (*25*). Structural figures were made with MOLMOL (*26*) and PyMOL (*27*).

Competitive Inhibition Assays Using Alanine Analogues of Pep.1. The coding sequence of the Hα1−205 fragment corresponding to residues 1−205 of the α-subunit of human nAChR was amplified by PCR using cDNA synthesized from total RNA extracted from the human TE671 cell line and cloned into the pET8C expression vector (*28*). Recombinant Hα1−205, present in the insoluble fraction, was dissolved in 9 M urea and then serially dialyzed against 50 mM Tris buffer (pH 8.0). Inhibition of mAb198 binding to nAChR was assayed as described previously (*28*). Briefly, microtiter plates were coated with Hα1−205 (5 μg/mL) in PBS and incubated overnight at 4 °C. After the solution was blocked with 1% BSA in PBS, mAb198 preincubated in the presence of different concentrations of peptide was added to the wells. Bound mAb198 was detected by incubation with horseradish peroxidase-conjugated goat anti-rat IgG (1:10000 dilution), followed by determination of horseradish peroxidase activity.

RESULTS

Peptide Synthesis. To determine how the structures of Pep.1 and Cyc.ext.Pep.1 relate to their different affinities for mAb198, Pep.1, a linear precursor of Cyc.ext.Pep.1, and hMIR were synthesized. Controlled air oxidation of the linear precursor was used for the folding of Cyc.ext.Pep.1, which entailed formation of a disulfide bond between the cysteines at both ends of the molecule. This process yielded satisfactory amounts of correctly folded oxidized compound on RP-HPLC (99% in the cyclized form, data not shown). Both the synthetic Pep.1 and Cyc.ext.Pep.1 had the expected molecular masses (1881 and 2675 Da) in MALDI-TOF analysis and gained 10.8 and 6.5 mg, respectively.

NMR Analysis and Determination of the Structure of Cyc.ext.Pep.1. We next carried out two-dimensional NMR analysis to investigate the structural characteristics underlying the increase in affinity for mAb198 that occurs in going from free Pep.1 to Cyc.ext.Pep.1. Complete sequence-specific resonance assignments for Cyc.ext.Pep.1 were determined using a standard protocol based on a set of traditional two-dimensional experiments (*29*). Identification of the amino acid spin system was based on scalar coupling patterns

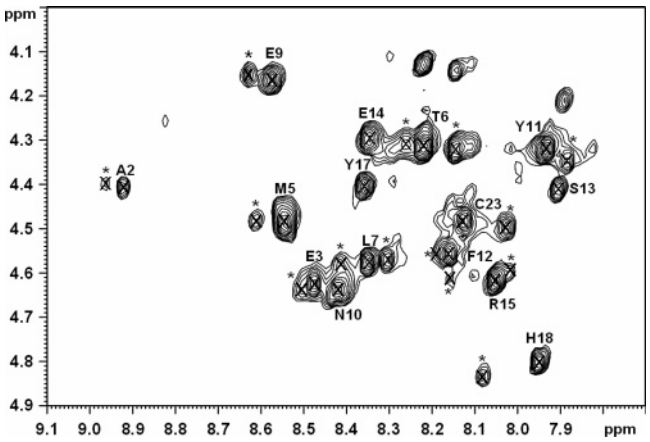

FIGURE 1: Fingerprint region of the TOCSY spectrum of 1 mM Cyc.ext.Pep.1 in PBS buffer (90% H_2O/10% D_2O) at pH 3.1. The TOCSY spectrum was acquired at the size of 256 (t_1) × 2048 (t_2) for 5 h at 298 K. Assigned NH−CαH cross-peaks are presented as single-letter amino acids and originate from the major form of Cyc.ext.Pep.1. Asterisks indicate cross-peaks originating from the minor form of Cyc.ext.Pep.1.

observed in DQF-COSY and TOCSY experiments, complemented by the results of NOESY measurements. The identified spin systems were sequentially assigned through inter-residue NOE connectivities observed in the NOESY spectrum. In the fingerprint region of Cyc.ext.Pep.1, almost all of the NH−CαH cross-peaks were observed as double peaks (Figure 1), indicating that Cyc.ext.Pep.1 assumes two different conformations in solution. Cross-peaks from the major form were shown with sufficiently strong intensity to be distinguished from the minor form. The presence of both a disulfide bond and Pro residues in the molecule likely underlies the conformational heterogeneity.

To calculate the structure of Cyc.ext.Pep.1, resonances of the major conformation were completely assigned and a total of 230 constraints were identified, including 222 distance constraints obtained from the interproton NOE cross-peaks, seven dihedral angle constraints from the coupling constraints, and one disulfide bond constraint. We executed the simulated annealing calculations beginning with 100 random Cyc.ext.Pep.1 structures and selected 16 final structures that were in good accordance with the NMR experimental constraints, which meant that the NOE distances and torsion angle violations were less than 0.3 Å and 3°, respectively. Statistics for the 16 converged structures were estimated using the structural parameters listed in Table 2. Within the 16 structures (Figure 2), the absence of distortions or unbonded bad contacts was checked using the small number of deviations from the idealized covalent geometry and the low values of the Lennard-Jones van der Waals energy. The average rms deviation from residue 7 to 19 was 2.20 ± 0.84 Å for the backbone atoms and 3.41 ± 1.16 Å for all heavy atoms. Outside the fitted region, the residues were not confined by the NMR constraints and the backbone was conformationally disordered. This reflects the scantiness of the NOE constraints, because of the flexibility of the side segments. Ramachandran analysis showed that the backbone dihedral angles were positioned within the proper regions.

The overall structure of Cyc.ext.Pep.1 contains several turn structures. Two type IV β-turn structures appear in the region of residues Pro8−Tyr11 and Pro20−Cys23, and a γ-turn structure is seen between Arg15 and Tyr17. Among these

Table 2: Structural Statistics for the Final 16 Structures of Cyc.ext.Pep.1

rms deviation from experimental distance constraints (Å)[a] (222)	0.0369 ± 0.0047
rms deviation from experimental dihedral constraints (deg)[a] (7)	0.3901 ± 0.2567
energetic statistics (kcal/mol)[b]	
F_{NOE}	0.0913 ± 0.0862
F_{tor}	6.2988 ± 0.7141
F_{repel}	14.9304 ± 3.7428
E_{L-J}	−32.9002 ± 6.2954
rms deviation from idealized geometry	
bonds (Å)	0.0034 ± 0.0003
angles (deg)	0.7385 ± 0.0234
impropers (deg)	0.4507 ± 0.0254
Ramachandran analysis (residues 7−19)[c]	
most favored regions	33.10%
additionally allowed regions	48.10%
generously allowed regions	18.80%
disallowed regions	0.00%
average rms deviations (Å) (residues 7−19)	
backbone (N, C^{α}, C)	2.20 ± 0.84
all heavy atoms	3.41 ± 1.16

[a] The number of each experimental constraint used in the calculations is given in parentheses. [b] F_{NOE}, F_{tor}, and F_{repel} are the energies related to the NOE violations, the torsion angle violations, and the van der Waals repulsion term, respectively. The values of the force constants used for these terms are the standard values listed in the X-PLOR 3.1 manual. E_{L-J} is the Lennard-Jones van der Waals energy calculated using the CHARMm empirical energy function. E_{L-J} was not used in the dynamically simulated annealing calculations. [c] PROCHECK_NMR was used to assess the stereochemical quality of the structures.

structural regions, the Pro8−Tyr11 and Arg15−Tyr17 regions are conserved in the sequences of Pep.1. Thus, addition of the flanking residues and disulfide bond constraints induced a rigid structure in the sequence of Pep.1.

To investigate the structure-related affinity difference between Pep.1 and Cyc.ext.Pep.1, we carried out a two-dimensional NMR analysis of free Pep.1, which revealed no medium- or long-range NOEs (data not shown), indicating that Pep.1 is very flexible. For that reason, instead of the structure of free Pep.1, we chose to examine the structure of the antigen epitope because the structural similarities and differences between Cyc.ext.Pep.1 and the antigen epitope could reveal the conformational dependence of Cyc.ext.Pep.1's affinity for mAb198.

NMR Analysis of mAb198-Bound Pep.1. To determine the structure of the antigen epitopes, we analyzed the structure of mAb198-bound Pep.1 in TRNOE experiments. With respect to their inhibition of mAb198 binding to Hα1−205, the IC_{50} values for Cyc.ext.Pep.1 and Pep.1 are ∼30 nM and ∼50 μM, respectively (*3*), which makes Pep.1 suitable for TRNOE experiments (*7*−*11*). The experiments with mAb198-bound Pep.1 were carried out with a mixing time of 150 ms without spin diffusion effects at a molar ratio of 1:10 for mAb198 and Pep.1. There was no difference in chemical shift from the intra and sequential NOEs at this ratio, and line broadening of the peptide resonance was observed in the one-dimensional ^{1}H NMR spectrum, indicating the binding of Pep.1 to mAb198 (*30*). Although the concentration of mAb198 was very low, the broadening effect of Pep.1 and the peaks of the antibody were apparent in the complex spectrum. As a result, the 2D TRNOE difference spectrum (*31*, *32*) could be obtained by subtracting the NOESY spectrum of mAb198 from that of the Pep.1−mAb198 complex.

Complete sequence-specific resonance assignments for the peptide were determined in the same way with Cyc.ext.Pep.1, but instead of a NOESY spectrum, we used the TRNOE difference spectrum for mAb198-bound Pep.1. Figure 3 shows the NH−CαH fingerprint region of the TRNOE difference spectrum for Pep.1, which includes sequential $d_{\alpha N}(i, i+1)$ connectivity. The pattern of observed transferred NOEs allowed us ultimately to identify the secondary structure of the molecule. Pep.1 bound to mAb198 exhibited several tight turns, and because medium- and long-range NOEs were only seen when Pep.1 was in the presence of mAb198, we knew that these structural properties were induced by the binding of Pep.1 to mAb198. In our comparison of the NOESY spectrum of free Pep.1 and the TRNOE difference spectra, we detected 16 cross-peaks caused by the structure of Pep.1 bound to mAb198: 12 cross-peaks were in the CH−NH regions of the TRNOE difference spectra (Figure 4); the others were related to the 9F δH−14Y NH, 15H NH−14Y NH, 5P δH−8Y βH, and 5P δH−4L βH interactions. In total, there were four cross-peaks of medium intensity, two of weak intensity, and 10 of very weak intensity. The 12 cross-peaks were representative of residues extending from Leu4 to Phe9, indicating that the rigid conformation in this region was mainly induced by interaction between Pep.1 and mAb198.

Determination of the Structure and Description of mAb198-Bound Pep.1. To calculate the structure of mAb198-bound Pep.1, we utilized 129 distance constraints derived from the two-dimensional TRNOE difference spectra, corresponding to an average of 9.2 constraints per residue. Of these, there were 85 intraresidue constraints, 34 interresidue constraints, and 10 dihedral angle constraints. We carried out the same processes with Cyc.ext.Pep.1 to obtain 20 final structures from 100 random structures of mAB198-bound Pep.1 (Figure 5A) and, using the structural parameters, estimated statistics for these 20 structures (Table 3). The average rms deviation in the region extending from residue 4 to 12 was 0.93 ± 0.32 Å for the backbone atoms and 2.05 ± 0.52 Å for all heavy atoms, and Ramachandran analysis showed that the backbone dihedral angles were positioned within the proper regions. The N-terminal (Pro1−Thr3) and C-terminal (Pro13−His15) segments were not restricted by NMR constraints so that the conformation of the backbone was randomly disordered. This may reflect a lack of medium- and long-range transferred NOE constraints due to flexibility resulting from deficient interaction between the peptide and antibody.

The molecular structure of mAb198-bound Pep.1 is characterized by tight turn structures. In the absence of antibody, Pep.1 has a flexible structure, which acquires its tight turns upon binding to mAb198. Two γ-turns are formed in the regions of residues Ser10−Arg12 and Arg12−Tyr14, though the last is not fixed due to insufficient medium- and long-range NOE constraints. In addition, one type IV β-turn structure is seen in the region between Pro5 and Tyr8. In the surface model of Pep.1 bound to mAb198, the region between Pro5 and Arg12 protrudes (Figure 5B) and contains two negatively charged acidic residues (Glu6 and Glu11), one positively charged basic residue (Arg12), and two bulky aromatic residues (Tyr8 and Phe9). Interestingly, Asn7 and Glu11 are in proximity upon binding to mAb198, causing the residues between Asn7 and Glu11 to be crowded into the functional patch. Within the fixed structural region of

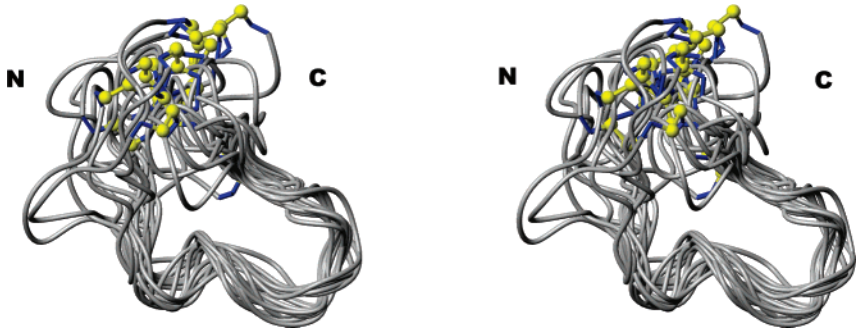

FIGURE 2: Stereoview of 16 converged structures of Cyc.ext.Pep.1. The central region between residues Leu7 and Pro19 was superimposed. The disulfide bond between Cys1 and Cys23 is illustrated using a ball and stick. This figure was generated using MOLMOL.

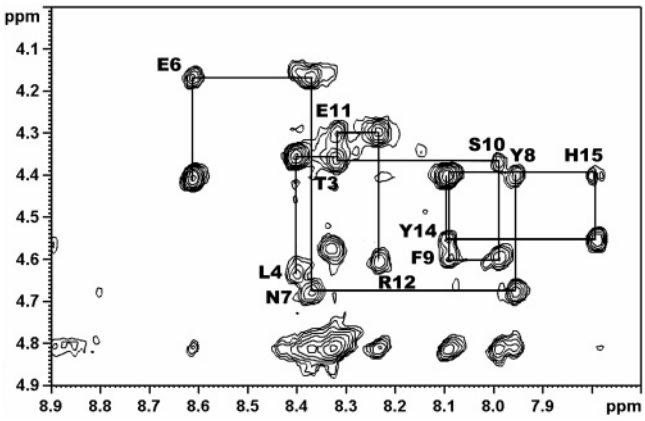

FIGURE 3: Sequential $d_{\alpha N}(i, i + 1)$ connectivities in the region extending from residue Thr3 to residue His15 in the TRNOE difference spectrum of mAb198-bound Pep.1 with a mixing time of 150 ms at 298 K. Intraresidue NH−CαH cross-peaks are presented using single-letter amino acid abbreviations.

mAb198-bound Pep.1, the regions between residue Pro5 and Tyr8 are consistent with the sequences of the structural regions of Cyc.ext.Pep.1. Moreover, residues Asn7 and Tyr8 in this common structural region are included in the protruding region.

Functional Characterization Using Competitive Inhibition Assays with Alanine Analogues of Pep.1. To determine which structural details of mAb-bound Pep.1 are relevant to affinity maturation of Cyc.ext.Pep.1, we defined the binding motifs of mAb198-bound Pep.1 using alanine scanning of Pep.1. Using an ELISA, we assessed the degree to which a set of Pep.1 analogues (1 mM), in which an alanine was sequentially substituted for each amino acid, could inhibit binding of mAb198 to Hα1−205. hMIR (1 mM) showed no inhibitory activity and served as a negative control for the assay (Figure 6A). Interestingly, the N7A and E11A analogues showed virtually no inhibitory activity (Figure 6A), suggesting hydrogen bonds with positively charged residues of mAb198 play key roles in the binding (*33*, *34*). The side chains of these residues were aligned in the same direction because of the close spacing of the two residues (Figure 6B). The inhibitory activities of the Y8A and F9A analogues were diminished by ∼80 and ∼72%, respectively, as compared to Pep.1. The side chains of these residues were extended in different directions from those of N7A and E11A (Figure 6B). These two bulky residues may participate in the hydrophobic interaction with the binding pocket of mAb198 (*33*, *34*). In addition, the inhibitory activity of the P5A analogue was diminished to ∼44% of the control, which might be indicative of its role in the induction of tight turn structures (*34*). Y14A and H15A analogues also inhibited the binding of mAb198 to Hα1−205 by ∼50%, though these two residues were outside of the structurally organized regions.

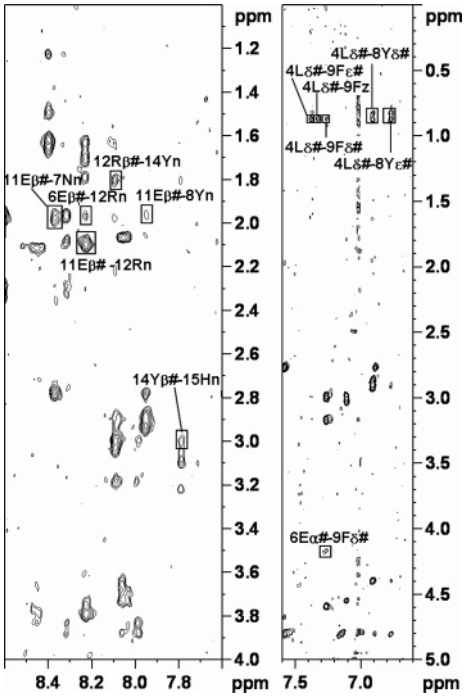

FIGURE 4: CH−NH regions in the TRNOE difference spectra of mAb198-bound Pep.1 (90% H_2O/10% D_2O, v/v). The TRNOE cross-peaks are labeled with the number of each residue and proton (#, pseudoatom). The water signal was suppressed using the WATERGATE scheme with field gradient pulses.

Within the structure of mAb198-bound Pep.1, important residues for the binding of Pep.1 to mAb198 are located in the tight turn structure and the protruding region and provide binding motifs for mAb198. Among the residues comprising the binding motifs, Asn7 and Tyr8 are in structural regions common to Cyc.ext.Pep.1 and mAb198-bound Pep.1. Moreover, these two residues overlapped upon structural superimposition of Cyc.ext.Pep.1 and mAb198-bound Pep.1 (Figure 7). Although Phe9, one of the important residues in the binding of Pep.1 to mAb198, is not positioned within the turn structures, this residue is also overlapped upon superimposition of the peptides. It thus appears that modification of Pep.1 to Cys.ext.Pep.1 causes structural similarities to develop between key residues of mAb198-bound Pep.1 and Cys.ext.Pep.1, and by satisfying the conformational

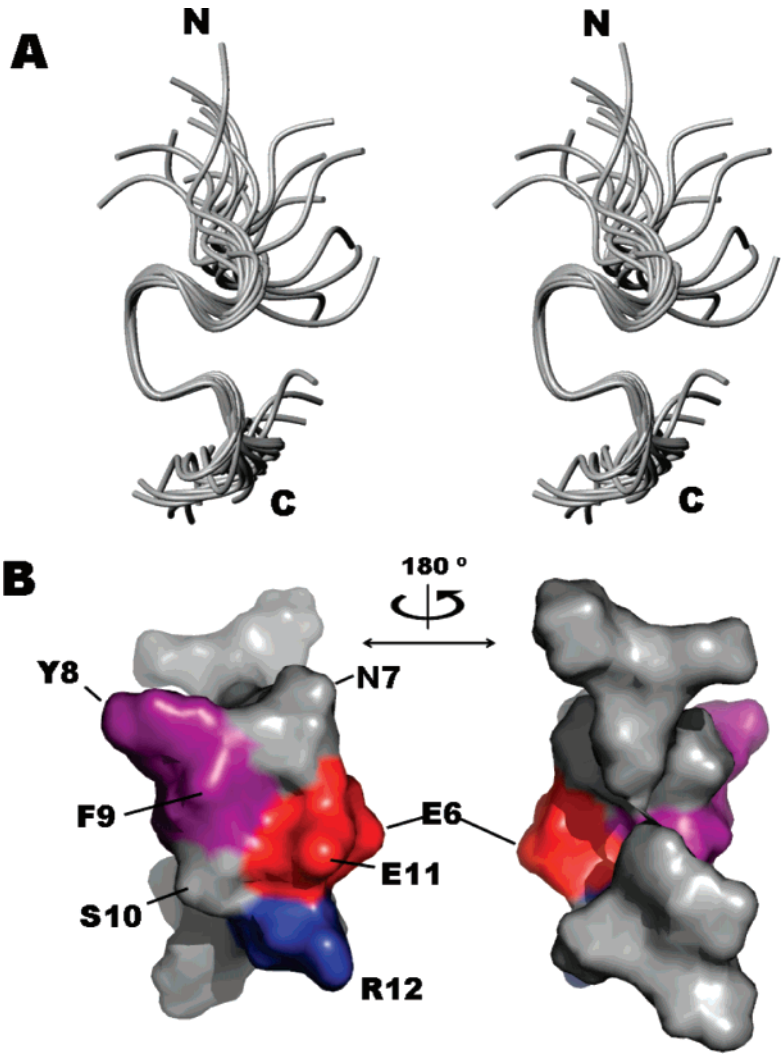

FIGURE 5: Structure of mAb198-bound Pep.1. (A) Stereopairs of the backbone heavy atoms of 20 converged structures of mAb198-bound Pep.1. All structures result from the best-fit superposition of residues 4−12 of Pep.1. This figure was made using MOLMOL. (B) Surface model of mAb198-bound Pep.1. Only in the protruded region (residues Glu6−Arg12) were the properties of each residue classified as hydrophobic (purple, Tyr8 and Phe9), basic (blue, Arg12), acidic (red, Glu6 and Glu11), or other (gray, Asn7 and Ser10). The two figures depict a 180° rotation about the vertical axis.

dependency of mAb198, these structural similarities mediate the increase in binding affinity for mAb198.

DISCUSSION

In a search for a therapeutic MG peptide mimotope, Pep.1 was identified from phage display libraries, but it proved to have limited affinity for the anti-MIR antibody mAb198 and failed to inhibit mAb198-mediated EAMG. By contrast, Cyc.ext.Pep.1 derived from Pep.1 has an affinity for mAb198 3 orders of magnitude greater than that of Pep.1 and successfully inhibited mAb198-mediated EAMG. In this study, we investigated the structure−affinity relationship between the peptides and elucidated the structural properties of free Pep.1, mAb198-bound Pep.1, and Cyc.ext.Pep.1. We showed that mAb198-bound Pep.1 and Cyc.ext.Pep.1 have structural similarities in their rigid turn structures, which contain important residues involved in mAb198 recognition, while free Pep.1 has a highly flexible structure.

Current treatment of autoimmune MG involves general immunosuppressive agents, which may have significant adverse side effects. An ideal therapy would specifically inhibit or eliminate the autoimmune response to nAChRs, without affecting the systemic immune system. Phage display technology could be a good method with which to screen candidate peptide mimotopes as target-specific neutralizing agents (*35*−*37*). Indeed, the peptides derived from phage display for inhibition of anti-MIR antibody would be advantageous in that they would specifically mimic the MIR region of the antigen (*38*, *39*) and thus neutralize disease-associated autoantibodies without affecting other facets of immune function. However, hMIR, a synthetic peptide corresponding to the MIR region of the nAChR α-subunit, was unable to neutralize the anti-MIR antibody because of its low affinity for the antibody. Eventually, however, the peptide library selected from the phage display system did exhibit the desired neutralizing activity (*3*). On the basis of this finding, in vitro affinity maturation was performed by incorporating flanking amino acid residues from the coat protein, which were present in the original phage library, yielding extended Pep.1 (ext.Pep.1), which showed a 10-fold increase in affinity over Pep.1 (*3*). Further addition of a cysteine residue at each end of the peptide and oxidation

Table 3: Structural Statistics for the Final 20 Structures of mAb198-Bound Pep.1

rms deviation from experimental distance constraints (Å)[a] (119)	0.0454 ± 0.0083
rms deviation from experimental dihedral constraints (deg)[a] (10)	0.9615 ± 0.3246
energetic statistics (kcal/mol)[b]	
F_{NOE}	0.6241 ± 0.3738
F_{tor}	2.6216 ± 0.4063
F_{repel}	3.6145 ± 1.2637
E_{L-J}	−29.0624 ± 8.6850
rms deviation from idealized geometry	
bonds (Å)	0.0030 ± 0.0002
angles (deg)	0.4506 ± 0.0429
impropers (deg)	0.3389 ± 0.0263
Ramachandran analysis (residues 4−12)[c]	
most favored regions	23.10%
additionally allowed regions	54.40%
generously allowed regions	22.50%
disallowed regions	0.00%
average rms deviations (Å) (residues 4−12)	
backbone (N, C^{α}, C)	0.93 ± 0.32
all heavy atoms	2.05 ± 0.52

[a] The number of each experimental constraint used in the calculations is given in parentheses. [b] F_{NOE}, F_{tor}, and F_{repel} are the energies related to the NOE violations, the torsion angle violations, and the van der Waals repulsion term, respectively. The values of the force constants used for these terms are the standard values listed in the X-PLOR 3.1 manual. E_{L-J} is the Lennard-Jones van der Waals energy calculated using the CHARMm empirical energy function. E_{L-J} was not used in the dynamically simulated annealing calculations. [c] PROCHECK_NMR was used to assess the stereochemical quality of the structures.

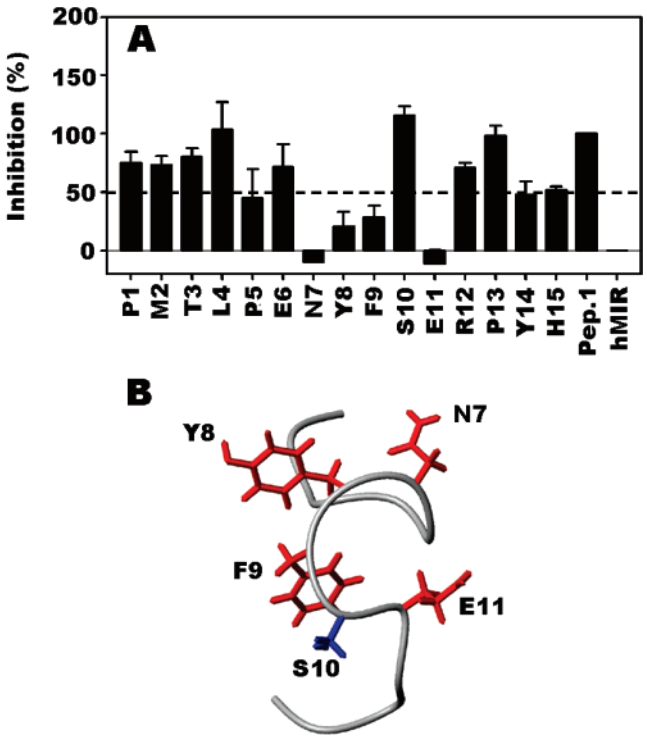

FIGURE 6: (A) Competitive inhibition assays for alanine-substituted Pep.1 analogues. Bars are labeled using the single-letter notation of each amino acid residue that had been substituted with alanine; hMIR refers to the MIR fragment (main immunogenic region, amino acids 67−76) from nAChR. The abilities of the analogues to inhibit the binding of mAb198 to Hα1−205 were normalized to the inhibitory activity of Pep.1, which was assigned a value of 100%. (B) Averaged structure of mAb198-bound Pep.1. The side chains of residues 7−11 are represented. The four functional residues are colored red, and the other is colored blue.

resulted in a cyclic peptide, Cyc.ext.Pep.1, which showed an affinity that was 3 orders of magnitude greater than that of the parent library peptide (*3*). However, no structure-related mechanism underlying the increased affinity was determined at that time. In this study, we show that incorporation of flanking resides and cyclization lead to structural changes in Pep.1 that mimic the spatial position of residues involved in the binding of Pep.1 to mAb198.

Pep.1 inhibited the binding of mAb198 to a human recombinant nAChR fragment, Hα1−205, more effectively than hMIR (*3*). This is because hMIR, which is comprised of residues 67−76 of the nAChR α-subunit, was not sufficient to mimic the conformation of the MIR region, as the fragment could not complete the folding processes that occurs in the intact protein. This study of the conformation of Pep.1 bound to mAb198 provided more information about the MIR region of nAChR and the structural characteristics of Pep.1 that compensate for the deficiencies of hMIR. Within the primary sequence of hMIR (WNPDDYGGIK), the PDDY stretch is homologous to the PENY stretch in Pep.1. In earlier studies of hMIR using synthetic peptides and site-directed mutants, residues Asn68, Asp70, Asp71, and Tyr 72 were shown to play important roles in the interaction between the nAChR α-subunit and mAb198 (*40*). Among them, Asp71 and Tyr72 are arranged in a homologous sequence, and Asn7 and Tyr8 of Pep.1, which were found to be important binding residues in competitive inhibition assays, could assume the roles of Asp71 and Tyr72 so that the formation of hydrogen bonds within hMIR (*34*, *41*) is compensated by these residues in Pep.1. The conformational change in Pep.1 that occurs upon mAb198 binding causes the side chains of Asn7 and Glu11 to be in the proximity of each other, which makes it possible to form hydrogen bonds that further contribute to affinity maturation. The hydrophobic interaction mainly involving residue Trp67 in hMIR (*34*) may be mediated by residue Phe9 in Pep.1, which can provide an interface for the hydrophobic interaction within the binding pocket of mAb198 (*34*). Although Pro5 of Pep.1 played a key role in inhibiting the binding of Pep.1 to mAb198, it may not make direct contact. Such is the case with Pro69 of hMIR (*34*), which also does not make contact with the antibody. This residue may be involved in the formation of the turn structure in the backbone of Pep.1 (*34*).

Pep.1 did not exhibit the same affinity for mAb198 as the phage presenting the Pep.1 sequence. Because Pep.1 is a linear form, it most likely does not have sufficient constraints to retain the structure necessary for binding to mAb198. By contrast, the phage-presented sequence apparently has enough constraints to stabilize a rigid structure within the Pep.1 sequence, resulting in an affinity higher than that of the linear form. Indeed, NMR analysis of Pep.1 in the absence of mAb198 showed it to be too flexible bind to mAb198, but addition of the flanking residues and disulfide bond constraints appears to cause it to imitate the phage construct (*3*, *42*). Because these modifications restrict the number of possible conformations and induce Cyc.ext.Pep.1 to have a conformation favorable to mAb198 binding, the entropic cost of forming a Cyc.ext.Pep.1−mAb198 complex is lower and the binding affinity of Cyc.ext.Pep.1 for mAb198 is higher than before modification. Cyc.ext.Pep.1 was produced by

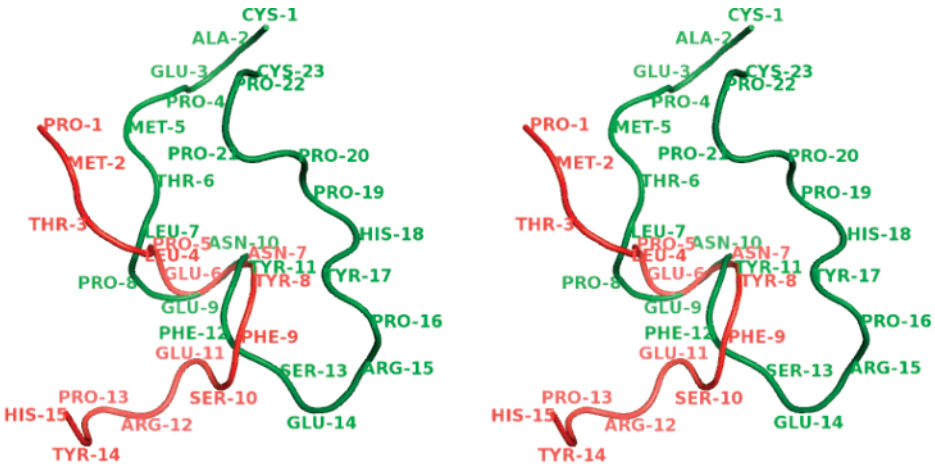

FIGURE 7: Average structures of mAb198-bound Pep.1 and Cyc.ext.Pep.1 were superimposed for comparison of the two peptides. The structure of mAb198-bound Pep.1 is colored red and that of Cyc.ext.Pep.1 green.

introducing residues, N-terminal (CAE) and C-terminal (PPPPC) sequences, and a disulfide bond between Cys1 and Cys23, resulting in a ring shape in which the added residues provide supplemental constraints to mimic the conformation of phage construct. By comparing the structures of mAb198-bound Pep.1 and Cyc.ext.Pep.1, we were able to determine how Cyc.ext.Pep.1 could have a structure similar to that of the antigen epitope. Figure 7 shows the effects of Pep.1 modification through superimposition of mAb198-bound Pep.1 and Cyc.ext.Pep.1. The region between residues Leu7 and Phe12 in Cyc.ext.Pep.1 overlapped to some extent with the Leu4−Phe9 region of mAb198-bound Pep.1. Within this region of Cyc.ext.Pep.1, turn structures were present between Pro8 and Tyr11, and the importance of residues Asn10 and Tyr11 was confirmed in competitive inhibition assays. Phe12 also is located within the region that overlaps when Cyc.ext.Pep.1 and mAb198-bound Pep.1 are superimposed and is likely involved in the affinity maturation of Pep.1, despite being outside the turn structure. On the other hand, Glu14 of Cyc.ext.Pep.1 was not arranged in structural agreement with the corresponding region of mAb198-bound Pep.1. It may be that conformational changes induced by the binding of Cyc.ext.Pep.1 to mAb198 cause Glu14 to assume a structural position that is spatially similar to that of Glu11 of mAb198-bound Pep.1. This possibility would likely reflect the rotational flexibility of the disulfide bond between Cys1 and Cys23.

In this study, we demonstrated how mimotopes like Pep.1 and Cyc.ext.Pep.1 interact with mAb198 at the atomic level. Moreover, we also determined why Cyc.ext.Pep.1 has a much higher affinity for mAb198 than its precursor, Pep.1: the rigid structure induced by incorporating flanking residues and cyclization mimics the structure of the antigen epitope within the nAChR (*3*, *42*), which increases the affinity of the peptide for mAb198. These findings indicate that the in vitro affinity maturation approach could be a general tool for enhancing the affinity of mimotopes developed to inhibit structure-dependent pathogenic autoantibodies such as those involved in MG. Ultimately, modification of peptide sequences based on structural aspects of the interaction between the autoantibody and peptide could enable development of immunotherapeutic peptides for use in the treatment of antibody-mediated autoimmune diseases.

ACKNOWLEDGMENT

We greatly thank Dr. S. J. Tzartos for permitting the use of mAb198.

REFERENCES

1. Fuchs, S. (1979) Immunology of the nicotinic acetylcholine receptor, *Curr. Top. Microbiol. Immunol. 85*, 1−29.
2. Drachman, D. B. (1996) Immunotherapy in neuromuscular disorders: Current and future strategies, *Muscle Nerve 19*, 1239−1251.
3. Venkatesh, N., Im, S. H., Balass, M., Fuchs, S., and Katchalski-Katzir, E. (2000) Prevention of passively transferred experimental autoimmune myasthenia gravis by a phage library-derived cyclic peptide, *Proc. Natl. Acad. Sci. U.S.A 97*, 761−766.
4. Tzartos, S. J., Barkas, T., Cung, M. T., Kordossi, A., Loutrari, H., Marraud, M., Papadouli, I., Sakarellos, C., Sophianos, D., and Tsikaris, V. (1991) The main immunogenic region of the acetylcholine receptor. Structure and role in myasthenia gravis, *Autoimmunity 8*, 259−270.
5. Barkas, T., Gabriel, J. M., Mauron, A., Hughes, G. J., Roth, B., Alliod, C., Tzartos, S. J., and Ballivet, M. (1988) Monoclonal antibodies to the main immunogenic region of the nicotinic acetylcholine receptor bind to residues 61−76 of the α subunit, *J. Biol. Chem. 263*, 5916−5920.
6. Tzartos, S. J., Kokla, A., Walgrave, S. L., and Conti-Tronconi, B. M. (1988) Localization of the main immunogenic region of human muscle acetylcholine receptor to residues 67−76 of the α subunit, *Proc. Natl. Acad. Sci. U.S.A 85*, 2899−2903.
7. Clore, G. M., and Gronenborn, A. M. (1982) Theory and applications of the transferred nuclear Overhauser effect to the study of the conformations of small ligands bound to proteins, *J. Magn. Reson. 48*, 402−417.
8. Campbell, A. P., and Sykes, B. D. (1991) Theoretical evaluation of the two-dimensional transferred nuclear Overhauser effect, *J. Magn. Reson. 93*, 77−92.
9. Clore, G. M., and Gronenborn, A. M. (1983) Theory of the time dependent transferred nuclear Overhauser effect: Application to the structural analysis of ligand-protein complexes in solution, *J. Magn. Reson. 53*, 423−442.
10. Johnson, M. A., Rotondo, A., and Pinto, B. M. (2002) NMR studies of the antibody-bound conformation of a carbohydrate-mimetic peptide, *Biochemistry 41*, 2149−2157.
11. Kim, J. I., Nagano, T., Higuchi, T., Hirobe, M., Shimada, I., and Arata, Y. (1991) Conformation and stereoselective reduction of hapten side chains in the antibody combining site, *J. Am. Chem. Soc. 113*, 9392−9394.

12. Merrifield, B. (1986) Solid phase synthesis, *Science 232*, 341−347.
13. Marion, D., and Wuthrich, K. (1983) Application of phase sensitive two-dimensional correlated spectroscopy (COSY) for measurements of ^{1}H-^{1}H spin-spin coupling constants in proteins, *Biochem. Biophys. Res. Commun. 113*, 967−974.
14. Bax, A., and Davis, D. G. (1985) MLEV-17-based two-dimensional homonuclear magnetization transfer spectroscopy, *J. Magn. Reson. 65*, 355−359.
15. Jeener, J., Meier, B. H., Bachmann, P., and Ernst, R. R. (1979) Investigation of exchange processes by two-dimensional NMR spectroscopy, *J. Chem. Phys. 71*, 4546−4553.
16. Macura, S., Huang, Y., Suter, D., and Ernst, R. R. (1981) Two-dimensional chemical exchange and cross-relaxation spectroscopy of coupled nuclear spins, *J. Magn. Reson. 43*, 259−281.
17. Piotto, M., Saudek, V., and Sklenar, V. (1992) Gradient-tailored excitation for single-quantum NMR spectroscopy of aqueous solutions, *J. Biomol. NMR 2*, 661−665.
18. Rance, M., Sorensen, O. W., Bodenhausen, G., Wagner, G., Ernst, R. R., and Wuthrich, K. (1983) Improved spectral resolution in cosy ^{1}H NMR spectra of proteins via double quantum filtering, *Biochem. Biophys. Res. Commun. 117*, 479−485.
19. Wuthrich, K., Billeter, M., and Braun, W. (1983) Pseudo-structures for the 20 common amino acids for use in studies of protein conformations by measurements of intramolecular proton-proton distance constraints with nuclear magnetic resonance, *J. Mol. Biol. 169*, 949−961.
20. Clore, G. M., Gronenborn, A. M., Nilges, M., and Ryan, C. A. (1987) Three-dimensional structure of potato carboxypeptidase inhibitor in solution. A study using nuclear magnetic resonance, distance geometry, and restrained molecular dynamics, *Biochemistry 26*, 8012−8023.
21. Pardi, A., Billeter, M., and Wuthrich, K. (1984) Calibration of the angular dependence of the amide proton-C α proton coupling constants, $^{3}J_{HN\alpha}$, in a globular protein. Use of $^{3}J_{HN\alpha}$ for identification of helical secondary structure, *J. Mol. Biol. 180*, 741−751.
22. Kline, A. D., Braun, W., and Wuthrich, K. (1988) Determination of the complete three-dimensional structure of the α-amylase inhibitor tendamistat in aqueous solution by nuclear magnetic resonance and distance geometry, *J. Mol. Biol. 204*, 675−724.
23. Brunger, A. T. (1992) A System for X-ray Crystallography and NMR, *X-PLOR Manual*, version 3.1, Yale University Press, New Haven, CT.
24. Laskowski, R. A., Rullmannn, J. A., MacArthur, M. W., Kaptein, R., and Thornton, J. M. (1996) AQUA and PROCHECK-NMR: Programs for checking the quality of protein structures solved by NMR, *J. Biomol. NMR 8*, 477−486.
25. Hutchinson, E. G., and Thornton, J. M. (1996) PROMOTIF: A program to identify and analyze structural motifs in proteins, *Protein Sci. 5*, 212−220.
26. Koradi, R., Billeter, M., and Wuthrich, K. (1996) MOLMOL: A program for display and analysis of macromolecular structures, *J. Mol. Graphics 14*, 51−55, 29−32.
27. DeLano, W. L. (2002) *The PyMOL molecular graphics system*, DeLano Scientific, San Carlos, CA.
28. Im, S. H., Barchan, D., Fuchs, S., and Souroujon, M. C. (1999) Suppression of ongoing experimental myasthenia by oral treatment with an acetylcholine receptor recombinant fragment, *J. Clin. Invest. 104*, 1723−1730.
29. Wuthrich, K. (1986) *NMR of Proteins and Nucleic Acids*, Wiley & Sons, New York.
30. Dwek, R. A. (1973) Nuclear Magnetic Resonance (NMR) in Biochemistry: Application to Enzyme Systems, Clarendon Press, Oxford, U.K.
31. Anglister, J., Levy, R., and Scherf, T. (1989) Interactions of antibody aromatic residues with a peptide of cholera toxin observed by two-dimensional transferred nuclear Overhauser effect difference spectroscopy, *Biochemistry 28*, 3360−3365.
32. Levy, R., Assulin, O., Scherf, T., Levitt, M., and Anglister, J. (1989) Probing antibody diversity by 2D NMR: Comparison of amino acid sequences, predicted structures, and observed antibody-antigen interactions in complexes of two antipeptide antibodies, *Biochemistry 28*, 7168−7175.
33. Poulas, K., Eliopoulos, E., Vatzaki, E., Navaza, J., Kontou, M., Oikonomakos, N., Acharya, K. R., and Tzartos, S. J. (2001) Crystal structure of Fab198, an efficient protector of the acetylcholine receptor against myasthenogenic antibodies, *Eur. J. Biochem. 268*, 3685−3693.
34. Kleinjung, J., Petit, M. C., Orlewski, P., Mamalaki, A., Tzartos, S. J., Tsikaris, V., Sakarellos-Daitsiotis, M., Sakarellos, C., Marraud, M., and Cung, M. T. (2000) The third-dimensional structure of the complex between an Fv antibody fragment and an analogue of the main immunogenic region of the acetylcholine receptor: A combined two-dimensional NMR, homology, and molecular modeling approach, *Biopolymers 53*, 113−128.
35. Devlin, J. J., Panganiban, L. C., and Devlin, P. E. (1990) Random peptide libraries: A source of specific protein binding molecules, *Science 249*, 404−406.
36. Cortese, R., Monaci, P., Luzzago, A., Santini, C., Bartoli, F., Cortese, I., Fortugno, P., Galfre, G., Nicosia, A., and Felici, F. (1996) Selection of biologically active peptides by phage display of random peptide libraries, *Curr. Opin. Biotechnol. 7*, 616−621.
37. Rodi, D. J., and Makowski, L. (1999) Phage-display technology: Finding a needle in a vast molecular haystack, *Curr. Opin. Biotechnol. 10*, 87−93.
38. Balass, M., Heldman, Y., Cabilly, S., Givol, D., Katchalski-Katzir, E., and Fuchs, S. (1993) Identification of a hexapeptide that mimics a conformation-dependent binding site of acetylcholine receptor by use of a phage-epitope library, *Proc. Natl. Acad. Sci. U.S.A. 90*, 10638−10642.
39. Barchan, D., Balass, M., Souroujon, M. C., Katchalski-Katzir, E., and Fuchs, S. (1995) Identification of epitopes within a highly immunogenic region of acetylcholine receptor by a phage epitope library, *J. Immunol. 155*, 4264−4269.
40. Tzartos, S. J., Barkas, T., Cung, M. T., Mamalaki, A., Marraud, M., Orlewski, P., Papanastasiou, D., Sakarellos, C., Sakarellos-Daitsiotis, M., Tsantili, P., and Tsikaris, V. (1998) Anatomy of the antigenic structure of a large membrane autoantigen, the muscle-type nicotinic acetylcholine receptor, *Immunol. Rev. 163*, 89−120.
41. Kozack, R. E., and Subramaniam, S. (1993) Brownian dynamics simulations of molecular recognition in an antibody-antigen system, *Protein Sci. 2*, 915−926.
42. Rudolf, M. P., Vogel, M., Kricek, F., Ruf, C., Zurcher, A. W., Reuschel, R., Auer, M., Miescher, S., and Stadler, B. M. (1998) Epitope-specific antibody response to IgE by mimotope immunization, *J. Immunol. 160*, 3315−3321.

BI701298B